Nonlinear computer-generated holograms

Asia Shapira,[1,*] Irit Juwiler,[2] and Ady Arie[1]

[1]*Department of Physical Electronics, School of Electrical Engineering, Tel Aviv University, Tel Aviv 69978, Israel*

[2]*Department of Electrical and Electronics Engineering, Sami Shamoon College of Engineering, Ashdod 77245, Israel*

**Corresponding author: asiasapi@post.tau.ac.il*

Received May 31, 2011; accepted June 28, 2011;
posted June 30, 2011 (Doc. ID 148444); published August 1, 2011

We propose a novel technique for arbitrary wavefront shaping in quadratic nonlinear crystals by introducing the concept of computer-generated holograms (CGHs) into the nonlinear optical regime. We demonstrate the method experimentally showing a conversion of a fundamental Gaussian beam pump light into the first three Hermite–Gaussian beams at the second harmonic in a stoichiometric lithium tantalate nonlinear crystal, and we characterize its efficiency dependence on the fundamental power and the crystal temperature. Nonlinear CGHs open new possibilities in the fields of nonlinear beam shaping, mode conversion, and beam steering.

OCIS codes: 190.2620, 090.2890.

Holography is a method for storing and reconstructing the amplitude and phase of a wavefront from an illuminated object [1]. Rather than using a real object, it was proposed in 1966 by Brown and Lohmann [2] to compute and print the required pattern of the hologram. When a light beam is sent through a computer-generated hologram (CGH), the far-field diffracted wavefront has the desired amplitude and phase. In 1967, Burch [3] described the following coding method for the amplitude transmittance function of a CGH:

$$t(x,y) = 0.5\{1 + A(x,y)\cos[2\pi f_{\text{carrier}}x - \varphi(x,y)]\}, \quad (1)$$

where $A(x,y)$ and $\varphi(x,y)$ are the amplitude and the phase, respectively, of the Fourier transform (FT) of the desired wavefront in the first diffraction order, and f_{carrier} is the frequency of the carrier function. $A(x,y)$ is normalized to the range 0–1, and $\varphi(x,y)$ is in the range 0–2π.

The ability to shape a generated wave in nonlinear conversion adds functionality and opens exciting new possibilities in nonlinear optics. For example, it enables all-optical self-routing and self-shaping of beams, whereby the obtained shape or direction depend on the phase-matching conditions [4,5]. Moreover, it should be noted that the alternative approach of shaping a beam in the fundamental frequency (FF) and then trying to frequency convert it would usually not work, except for some very simple cases [6], owing to the difficulties of maintaining the phase-matching requirements with non-Gaussian beams. Previous demonstrations of nonlinear beam shaping relied on varying the interaction length [7], on introducing a transverse-dependent phase term in a periodic structure [4,8], on a nonlinear structure that generated multiple focal points at the converted frequency [9], or on nonlinear wave mixing [10]. However, none of these provided a full amplitude and phase control.

In this Letter we extend, for the first time to our knowledge, the concept of CGH into the nonlinear optical regime. In this case, the second-order nonlinear coefficient of a crystal is modulated, so that when a fundamental light beam passes through it, a wavefront with the chosen amplitude and phase is obtained in the second harmonic (SH). Unlike its linear counterpart, a challenge that appears in the nonlinear CGH is the requirement for phase-matching of the interacting waves. Moreover, the main method for modulating the nonlinear coefficient—electric field poling in ferroelectric crystals [11]—is a planar method that enables us to utilize only two out of the three available axes of the nonlinear crystal. The solution we have devised for overcoming these limitations is to use one axis—the propagation axis for quasi-phase-matching, while using one of the transverse axes for imposing the amplitude and phase modulation. The two-dimensional modulation of the second-order nonlinearity coefficient of a nonlinear crystal is therefore

$$\chi^{(2)}(x,y) = d_{ij}\text{sign}\{\cos[2\pi f_{\text{QPM}}x + \pi t(y)]\}, \quad (2)$$

where d_{ij} is an element of the quadratic susceptibility $\chi^{(2)}$ tensor, f_{QPM} is the spatial frequency of the quasi-phase-matching in the beam's propagation direction, and $t(y)$ is the one-dimensional equivalent of Eq. (1), i.e.,

$$t(y) = 0.5\{1 + A(y)\cos[2\pi f_{\text{carrier}}y - \varphi(y)]\}. \quad (3)$$

To demonstrate the concept of encoding a CGH in nonlinear crystals, we chose to fabricate a crystal aimed to generate the first three modes in the Hermite–Gaussian (HG) family [12], HG_0, HG_1, and HG_2, in the first diffraction order. The spatial distribution of HG modes propagating in the x direction, which are plane waves in the z direction and HG modes in the y direction, is

$$U_m(y,x) = A_m\frac{W_0}{W(x)}G_m\left[\frac{\sqrt{2}y}{W(x)}\right] \times \exp\left[-ikx - ik\frac{y^2}{2R(x)} + i(m+1)\xi(x)\right], \quad (4)$$

where A_m is the amplitude and W_0 and $W(x)$ are the waist and local beam radii, respectively, $G_m(u)$ is the mth-order HG function, k is the wave vector, $R(x)$ is the beam curvature, and ξ is the Gouy phase. Because the FT of an HG mode is the same HG mode, $t(y)$ was calculated according to Eq. (4). A schematic illustration of the proposed experimental setup is shown in Fig. 1; parts (a)–(c)

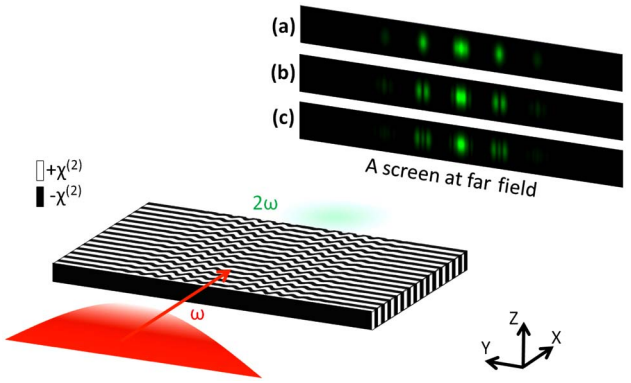

Fig. 1. (Color online) Schematic illustration of the nonlinear CGH setup. Simulation results at the far field for (a) HG_0, (b) HG_1, and (c) HG_2.

in the figure show simulations of the far-field images for each one of the modes.

We fabricated the suggested structure by two-dimensional electric field poling of a stoichiometric lithium tantalate nonlinear crystal. The modulation period in the propagation direction, $1/f_{\mathrm{QPM}}$, was 7.87 μm, designed to phase-match an e-ee SH generation of a 1064.5 nm Nd:YAG laser at 100 °C [13]. The duty cycle of the crystal was 30%. The crystal had three separate 2.5 mm wide channels, with different modulations of the second-order nonlinearity coefficient, with $t(y)$ corresponding to the three desired HG modes [Eq. (4)]. The length of the channel designed for HG_0 was 7.5 mm, and the lengths of the other two channels were 10 mm. The FF source used was a Nd:YAG laser producing 10 ns pulses at a 2 kHz repetition rate at a wavelength of 1064.5 nm. An extraordinary polarized laser beam was focused to the center of the crystal with a cylindrical lens, creating a waist radius of approximately 60 μm and 1 mm in the crystallographic z and y directions, respectively. An additional cylindrical lens was placed at the output of the crystal.

The desired HG modes were obtained at the first (left and right, +1 and −1) diffraction order. The frequency of modulation in the y direction, f_{carrier}, was chosen to be 0.0089 $\mu\mathrm{m}^{-1}$, hence the first diffraction order is obtained at an external angle of $\lambda_{\mathrm{SH}} f_{\mathrm{carrier}} \sim 4.7$ mrad, where λ_{SH} is the SH wavelength. Figure 2 presents a comparison between the theoretical and the measured profiles in the first diffraction order of the three channels in the crystal.

A detailed comparison between the experimental and simulated results for the HG_1 beam is presented in Fig. 3. Numerical simulation was performed based on the split-step Fourier method, with physical parameters identical to the ones in the experiment and assuming $d_{33} = 12.9$ pm/V [13]. We examined both the total SH

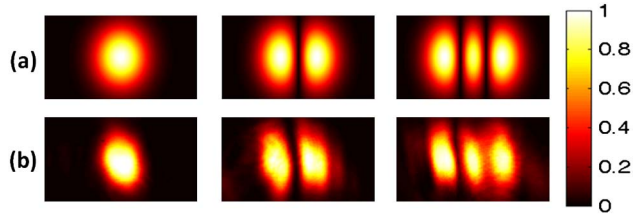

Fig. 2. (Color online) Comparison between (a) theoretical and (b) measured beam profiles at the first diffraction order.

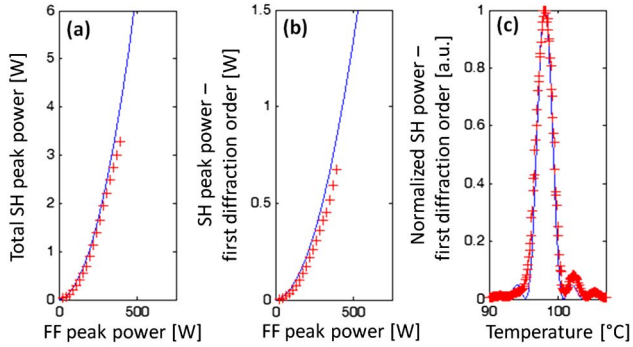

Fig. 3. (Color online) Comparison between measured (plus-sign curves) and predicted (solid curves) results: (a) total output power dependence on input power, (b) diffracted output power dependence on input power, and (c) diffracted output power dependence on temperature.

generation and the power of the first diffraction order as a function of the input FF power, as shown in Figs. 3(a) and 3(b). The results indicate that approximately 20% of the total SH power is, in each one of the two beams, generated in the first diffraction order. A good agreement was also found between the simulated and the measured conversion efficiencies of the examined beams, thereby indicating that the quality of modulation provided by the electric field poling technique is sufficient for realization of nonlinear CGHs. The comparison between the simulated and measured efficiencies for the three CGHs is given in Table 1. It is interesting to note that the predicted conversion efficiency for a conventional 10 mm long one-dimensional periodically poled structure under the same experimental configuration is $2.4 \times 10^{-3}\ \%\mathrm{W}^{-1}$, i.e., the same as we observed for the holograms that generated the HG_1 and HG_2 modes. This is in fact expected, because the modulation along the Y axis does not affect the conversion efficiency of the crystal.

We also checked the temperature dependence of the nonlinear process—a comparison between measured and simulated results is presented in Fig. 3(c). The simulated result was shifted by 2 °C to fit the measured result; a good agreement is seen between the two curves, thereby indicating that the process is phase matched over the entire length of the crystal.

In order to validate that the measured beams at the first diffraction order are indeed HG beams, we evaluated the M^2 values of the beams. The M^2 of a diverging beam can be calculated using the relation $W_y^2(x) = W_{0y}^2 + (M_y^2)^2(\lambda/\pi W_{0y})^2(x - x_0)^2$, where W_y is twice the standard deviation (σ_y), which is calculated from the second moment of the transverse distribution; x_0 and W_{0y}

Table 1. Comparison between Predicted and Measured Conversion Efficiencies for the Total and the Diffracted Second Harmonic

Mode	Prediction		Measurement	
	Total SH [$\%\mathrm{W}^{-1}$]	Mode SH [$\%\mathrm{W}^{-1}$]	Total SH [$\%\mathrm{W}^{-1}$]	Mode SH [$\%\mathrm{W}^{-1}$]
HG_0	1.5×10^{-3}	3×10^{-4}	1.3×10^{-3}	2.2×10^{-4}
HG_1	2.4×10^{-3}	5.1×10^{-4}	1.8×10^{-3}	4.2×10^{-4}
HG_2	2.4×10^{-3}	5.1×10^{-4}	2×10^{-3}	3.9×10^{-4}

Table 2. Comparison between Theoretical and Measured M^2 for the Generated Modes

Mode	Theory	Measurement
HG_0	1	1.69 ± 0.08
HG_1	3	3.27 ± 0.16
HG_2	5	5.21 ± 0.22

are the waist location and size, respectively; and λ is the wavelength. The transverse profiles were measured with a laser beam profiler at the waist, and a few Rayleigh lengths away, $2\sigma_y$ values were estimated calculating the second moment of the measured profiles. The evaluated M^2 of the Gaussian FF beam is 1.21 ± 0.012. Table 2 summarizes the results of the evaluated values of M^2 for the different SH beams; a fair agreement is seen between the evaluated and theoretical results. The difference between the values may originate from the ellipticity of the modes due to the elliptical shape of the FF beam.

Nonlinear CGHs can be used to generate arbitrary shapes of beams and are not limited only to HG beams. An additional example of implementing the suggested nonlinear CGH is the generation of one-dimensional accelerating Airy beams [14]. Figure 4 presents simulation results of the output of an Airy nonlinear CGH. The crystal is assumed to be 10 mm long, with a duty cycle of 50%; the frequency of modulation in the y direction, f_{carrier}, is $0.0145\,\mu\text{m}^{-1}$. As can be seen, two Airy beams are generated in the $+1$ and -1 diffraction orders. The first diffraction order is obtained at an external angle of $\lambda_{\text{SH}} f_{\text{carrier}} \sim 8$ mrad, and the total phase deviation imposed on a 1.4 mm wide beam is -16π to 16π. Figure 4(a) shows the SH normalized power at the focal plane of a 125 mm lens placed to perform an optical spatial FT of the crystals output. Figure 4(b) shows the propagation of the left Airy beam. The well-known features of this beam, acceleration and slow diffraction, are clearly observed. Figure 4(c) is a schematic illustration of the poling pattern of the nonlinear crystal. The predicted internal conversion efficiency for a single Airy beam in this case is $3.1 \times 10^{-3}\,\%\text{W}^{-1}$, for an elliptical beam with a waist radius of 45 μm and 0.7 mm in the crystallographic z and y directions, respectively. Previously, we have generated nonlinear Airy beams using an asymmetric nonlinear photonic crystal [4]. The nonlinear CGH has the advantage of providing two Airy beams instead of one. Furthermore, these beams are separated from the fundamental beam that remains mainly in the zeroth diffraction order.

The suggested nonlinear CGH in this Letter enables one-dimensional shaping of the wavefront in the first diffraction order; however, the concept of the nonlinear CGH can also be implemented for two-dimensional shaping by combining a transverse setting of a two-dimensionally poled nonlinear crystal [15] with binary CGH coding [16].

In conclusion, we have extended the idea of CGHs to nonlinear quadratic crystals and experimentally demonstrated the concept, for the first time to our knowledge,

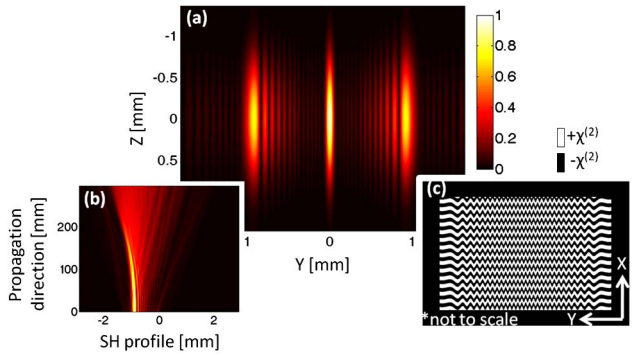

Fig. 4. (Color online) (a) Simulation of a one-dimensional Airy beam generation with a nonlinear CGH, normalized SH output power at the focal plane of a 125 mm lens placed after the crystal, (b) propagation of the generated Airy beam, and (c) schematic illustration of the modulation of the nonlinear coefficient in the suggested nonlinear CGH.

by converting a fundamental HG_0 Gaussian beam pump light into the first three HG beams at the SH. Furthermore, we demonstrated that nonlinear optical beam shaping can be employed for any desired wavefront. The ability to efficiently convert the frequency of light and to reshape its wavefront will be useful for all-optical shaping, routing, and switching of beams.

This work was supported by the Israel Science Foundation (ISF), under grant 774/09. The authors thank Soreq NRC for the assistance with the poling of the crystal.

References

1. D. A. Gabor, Nature **161**, 777 (1948).
2. B. R. Brown and A. W. Lohmann, Appl. Opt. **5**, 967 (1966).
3. J. J. Burch, Proc. IEEE **55**, 599 (1967).
4. T. Ellenbogen, N. Voloch-Bloch, A. Gannay-Padowicz, and A. Arie, Nat. Photon. **3**, 395 (2009).
5. I. Dolev, T. Ellenbogen, and A. Arie, Opt. Lett. **35**, 1581 (2010).
6. I. Dolev and A. Arie, Appl. Phys. Lett. **97**, 171102 (2010).
7. G. Imeshev, M. Proctor, and M. M. Fejer, Opt. Lett. **23**, 673 (1998).
8. J. R. Kurz, A. M. Schober, D. S. Hum, A. J. Saltzman, and M. A. Fejer, IEEE J. Sel. Top. Quantum Electron. **8**, 660 (2002).
9. Y. Qin, C. Zhang, Y. Zhu, X. Hu, and G. Zhao, Phys. Rev. Lett. **100**, 063902 (2008).
10. T. Ellenbogen, I. Dolev, and A. Arie, Opt. Lett. **33**, 1207 (2008).
11. M. Yamada, N. Nada, M. Saitoh, and K. Watanabe, Appl. Phys. Lett. **62**, 435 (1993).
12. B. E. A. Saleh and M. C. Teich, *Fundamentals of Photonics* (Wiley, 1991).
13. I. Dolev, A. Ganany-Padowicz, O. Gayer, A. Arie, J. Mangin, and G. Gadret, Appl. Phys. B **96**, 423 (2009).
14. G. A. Siviloglou, J. Broky, A. Dogariu, and D. N. Christodoulides, Phys. Rev. Lett. **99**, 213901 (2007).
15. V. Berger, Phys. Rev. Lett. **81**, 4136 (1998).
16. W. H. Lee, Appl. Opt. **18**, 3661 (1979).